SSRG International Journal of Applied Physics
ISSN: 2350-0301/ https://doi.org/10.14445/23500301/IJAP-V10I1P104

Volume 10 Issue 1, 22-33, Jan-Apr 2023

Original Article

Reporting Phase Transitions of a New Generation "Tertiary Liquid Crystal System" (TLCS) using Logger Pro

Medaelle Seide[1], Dipti Sharma[2]

[1,2]*Department, Chemistry and Physics, Emmanuel College, Boston, MA, USA*

[2]*Corresponding Author : dsharmaphd@gmail.com*

Received: 10 March 2023 Revised: 12 April 2023 Accepted: 24 April 2023 Published: 30 April 2023

Abstract *- This paper reports details of phase transitions of a new generation "Tertiary Liquid Crystal System" (TLCS). This TLCS was made with a mixture of 5CB, 6CB, and 7CB liquid crystals. The TLCS was run in DSC to find changes taking place in its heat flow as a function of time and temperature analyzed with Logger Pro. The sample of TLCS was run from -40 °C to 80 °C with a 20 °C/min ramp rate in DSC. It was observed that the TLCS shows two phase transitions on heating and one transition on cooling. All these transitions were found to shift when compared to their single members. The unique behavior of TLCS is that it never shows crystallization in cooling, even though the sample was cooled to -40 °C. This indicated an increase in its Nematic range, making it more useful in the Liquid Crystal Display (LCD) field.*

Keywords *- Liquid Crystals (LCs), Differential Scanning Calorimetry (DSC), Tertiary Liquid Crystal System (TLCS), Heat, Cool, Ramp rate, LoggerPro, Heat Flow, Specific Heat Capacity, Temperature, Crystallization, Nematic, Isotropic, Melting, Frozen Nematic, Endothermic, Exothermic, 1st derivative, 2nd derivative, 3rd derivative.*

1. Introduction

During the 19th century, Otto Lehman and Friedrich Reinitzer recognized the concept of Liquid Crystals (LCs) as a fourth state of matter. These substances show the unique properties of solid and liquid states. The molecules' alignment can be changed based on the temperature. During the cooling process, the isotropic to nematic transition occurs when the molecules are usually randomly oriented, which is like how they are in traditional liquids. However, after cooling, the system transitions to the nematic phase. This occurs when the molecules follow a common direction. While maintaining a liquid state, a liquid crystal can polarize light by changing its vertical or horizontal orientation. [1-3] This process can also be performed by using electric fields to alter the light's effect depending on the phase of the crystal. Due to the use of blocking light, Liquid Crystal Displays (LCDs) came into the market in the form of Liquid Crystal devices that are significantly compact and use less energy. Instead of producing light, they use LCs to create high-resolution images. In LCDs, when illuminated by a backlight, the pixels switch on and off while the crystal rotates the light to produce a certain colour. Each pixel is sandwiched between a glass filter and a polarizing glass. [7-26]

During the 20th century, liquid crystals (LCs) were instrumental in developing information display technology.

However, in the 21st century, their applications have become more sophisticated. In addition to being utilized in various electronic devices, such as televisions and computers, liquid crystals are also being used in navigation systems, smartphones, and other gadgets. Every monitor pixel has an orientation-changing electromagnetic field, which acts as a conductor between the light and the liquid crystals. Liquid crystals are a unique material class that exhibits properties between conventional liquid and solid matter. Their unique characteristics have made them indispensable in the advancement of modern technology. [1-7]

Liquid crystals exhibit different phases of matter ranging from solid to liquid states. The molecular arrangement of these materials changes as temperature changes, which can be studied using DSC. [8-9]

For decades, the Differential Scanning Calorimetry (DSC) technique has been used to analyze the thermal behaviour of different materials. [10-15] It can be used to study and detect changes in states due to different factors, such as exothermic or endothermic peaks. It can also be used to observe changes in the heat flow of the sample. [16-20] By studying the phase transitions that occur, researchers can gain a deeper understanding of how these materials function. Several studies have been performed using DSC, and some of them can be seen here. [10-25]

LCs have been studied by various authors and researchers for decades, either as a single LC or a combination of LCs. The binary liquid crystals can be formed by mixing two pure liquid crystals together at a certain ratio. Some studies can be found on Binary LCs. One example can be seen when 5CB and 7CB are mixed, and it goes from crystallization to Isotropic during heating. When it is cooled, it goes to nematic from isotropic but never goes back to crystallization. [10] Because of this strange behavior of Binary LCs, our interest increases in Tertiary LCs.

The most distinctive difference between tertiary and binary liquids crystals is the number of different types of LCs that are mixed. Liquid crystals have gained significant attention due to their numerous applications in the field of materials science, particularly in electronic display technologies such as liquid crystal displays (LCDs). Understanding the phase transitions in liquid crystals is crucial for developing and optimizing these materials for various applications. This research will provide an in-depth analysis of tertiary liquid crystals, their properties, and their significance in their application in smart devices. This paper reports details of the phase transition of Tertiary LCs where three LCs are mixed and then run in DSC to find details of it.

2. Materials and Methods

Three liquid crystals from the nCB family were used for the study. These are three pure, bulk samples of 4'-Heptyl-4-cyanobiphenyl (7CB), 4-Hexyl-4'-cyanobiphenyl (6CB), and 4-pentyl-4-cyanobiphenyl (5CB) LCs. These LCs are mixed in a ratio of 1:1:1. The chemical structure of these LCs can be seen in Figure 1.

The molecular weight of these three LCs is given as s of 249.36, 263.38, and 277.41 g/mol, respectively. These three LCs were taken in equal amounts and then mixed to make a mixture of three LCs. They are then heated to a little over to their Isotropic temperature to get a full melt of the mixture for about an hour and get stirred. Then they were cooled and used for studying. We call this mixture of threes "Next Generation Liquid Crystals" as they bring some unique changes in their phase transitions. We also like to call this mixture a "Tertiary Liquid Crystal System" (TLCS), as this sample is a mixture of three LCs from the same family with three different tail sizes but the same functional group. All of them have a cyano group, a benzene group, and a tail of C-H. Hence the TLCS, in short, is 5CB + 6CB + 7CB (1:1:1). Here is the cartoon of these three LCs showing their oval shape with three different sizes in Figure 2. The 5CB, 6CB and 7CB have 5CH, 6CH, and 7CH groups in their tails.

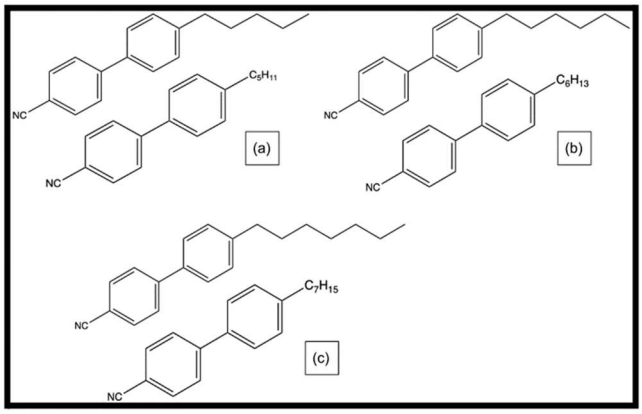

Fig. 1 Skeletal and simplified chemical structure of LCs (a) 5CB, (b) 6CB, (c) 7CB.

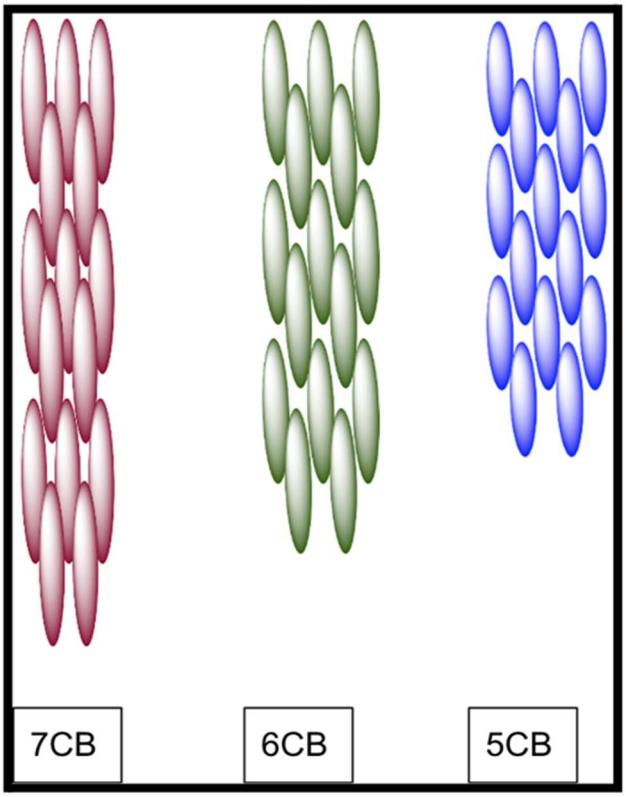

Fig. 2 Molecular sizes of 5CB, 6CB, and 7CB.

After making this TLCS, a small amount was taken to an advanced Differential Scanning Calorimeter (DSC) from the NETZSCH company with model DSC 214 located at the chemistry and biochemistry department of WPI. The sample of 5CB+6CB+7CB was then run from -40 °C to 80 °C and then back from 80 °C to -40 °C with a 20 °C/min ramp rate. The DSC instrument gave DSC thermograms with data for heat flow versus time and temperature. The data was collected from DSC and then taken to Logger Pro for detailed analysis to find details of phase transitions of this TLCS.

3. Theory

The materials The DSC instrument follows thermodynamics and does thermal analysis of the samples used in it. The Heat Flow goes to the sample as temperature increases, and the instrument records the change in heat flow as the sample moves temperature. The relationship between heat flow (dQ/dt) and heating rate (dT/dt) can be seen in equation 1, where mass (m) and specific heat capacity (Cp) of the substance also have a connection with it.,

$$\frac{dQ}{dT} = m * Cp * \frac{dT}{dt} \quad (1)$$

The specific heat capacity of the sample can be found by equation 2,

$$Cp = \frac{1}{m} * \left(\frac{dQ}{dt} / \frac{dT}{dt}\right) \quad (2)$$

The heat absorbed during transitions can be found in terms of Enthalpy (ΔH) and can be found from equation 3.

$$\Delta H = \int Cp\, dt \quad (3)$$

Since the heat flow as a function of time shows how slow and fast heat flows into the sample with time or flowing out of the sample with time, the thermal speed, thermal acceleration, and thermal jerk can also be calculated from heat flow. These details can be seen in the following equations below. These equations show that derivatives of heat flow (HF) can be used for that, shown in equation 4.

$$HF = m * C * \frac{dT}{dt} = \frac{dQ}{dt} \quad (4)$$

The first derivative of the HF gives the thermal speed (v) shown in Equation 5, which gives the change in heat flow over a given time ($\frac{d(HF)}{dt}$).

$$v = \frac{d(HF)}{dt} = m * C * \frac{d^2(Q)}{dt^2} \quad (5)$$

The second derivative of the heat flow equation gives the Thermal acceleration (a) shown in equation 6.

$$a = m * C * \frac{d^3(Q)}{dt^3} \quad (6)$$

$$J = m * C * \frac{d^4(Q)}{dt^4} \quad (7)$$

In a similar way, the third derivative of the heat flow equation gives the thermal jerk (J), shown in equation 7.

4. Results

The data obtained from DSC was then taken to the Logger Pro to plot graphs for this TLCS. The details of the graphs are shown in this section.

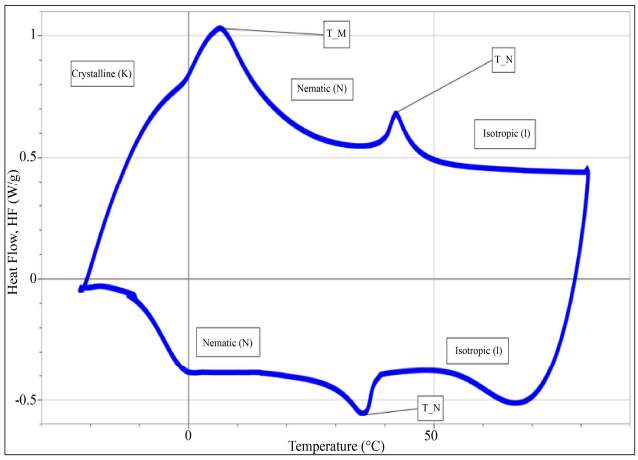

Fig. 1 Heat Flow (HF) vs Temperature (T) plot of the Crystalline (K), Nematic (N), and Isotropic (I) phase transitions of TLCS for the heating and cooling cycle.

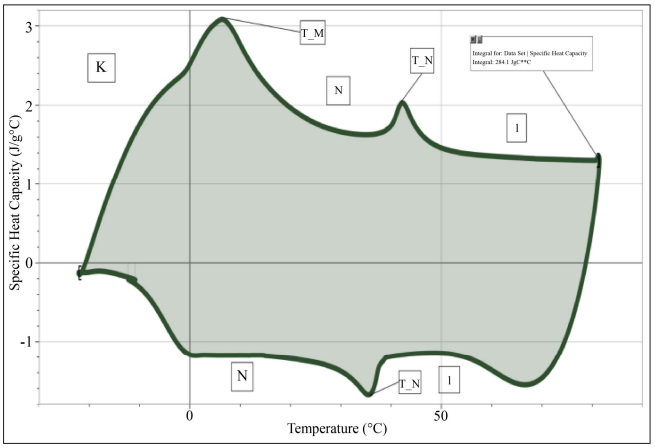

Fig. 2 Specific Heat Capacity (Cp) Vs. Temperature plot of TLCS. The shaded area represents the change in internal energy of the TLCS mixture during heating and cooling.

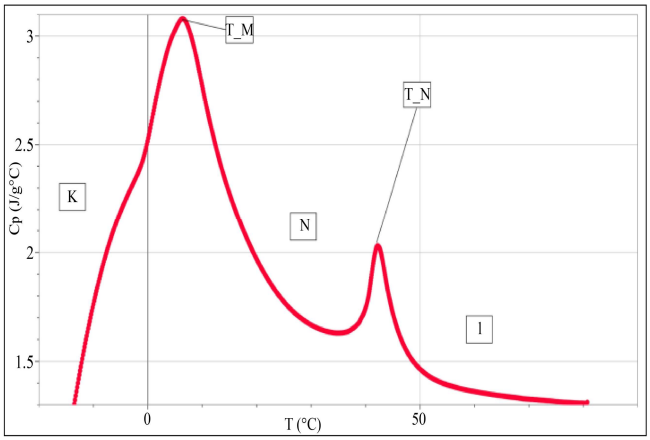

Fig. 3 The phase traditions occur during the heating process of the TLCS

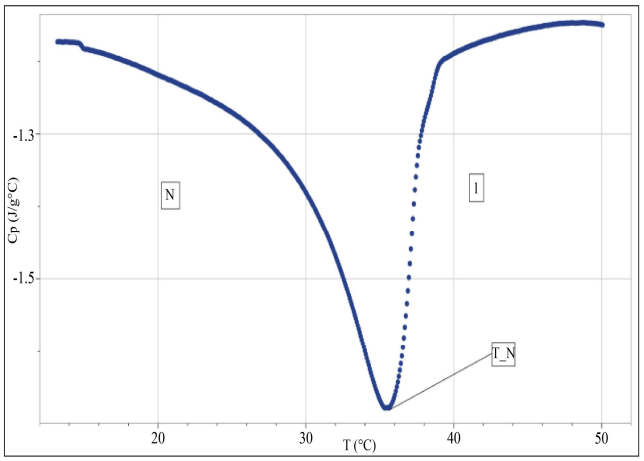

Fig. 4 The phase transition occurs during the cooling of the TLCS.

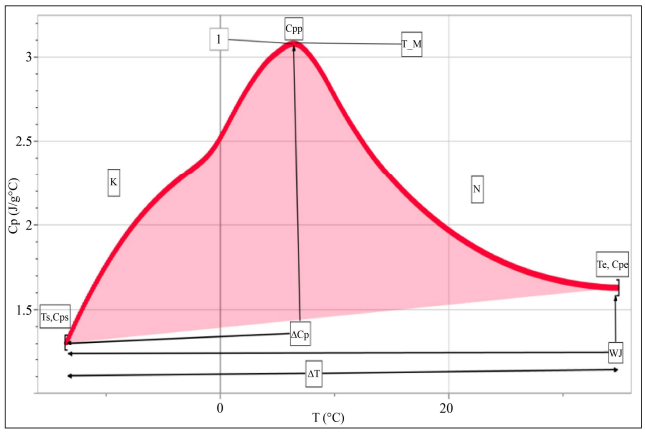

Fig. 5 The Cp Vs Temperature (T) for the endothermic melting peak of the TLCS.

Figure 2, Cp vs T, shows how much internal energy was used by the TLCS during the heating and cooling process. The green shaded area shows the integral of the plot, which is the total energy increased within the TLCS during heating and cooling. The internal energy increased during the cycle was 284.1 J/g°C.

Figure 3, Cp vs T, shows the endothermic melting and nematic transition peaks on heating, showing how much energy is absorbed by the TLCS molecules. Moreover, Figure 4, Cp vs T, shows the exothermic nematic transition peak during cooling and shows how much energy is released from TLCS molecules.

Figure 5 shows the enlarged melting phase transition peak of the TLCS. It highlights the starting and ending temperatures along with their corresponding specific heat capacity value. The Cp peak, wing jump, change in temperature, and change in specific heat capacity of the melting phase transition are identified. The pink shaded area represents the peak integral, which calculates the amount of energy used for the melting transition. The amount of thermal energy required for the melting transition was 34.05 J/g. The symbols used are recorded in Table 2.

Figure 6 shows the enlarged endothermic nematic phase transition peak of the TLCS. It highlights the starting and ending temperatures along with their corresponding specific heat capacity value. The Cp peak, wing jump, change in temperature, and change in specific heat capacity of the melting phase transition are identified. The pink shaded area represents the peak integral, which calculates the amount of energy used for the melting transition. The amount of thermal energy required for the melting transition was 2.48 J/g. The symbols used are recorded in Table 2.

Figure 8 shows HF vs t plot for TLCS for heating only. Figure 9 shows the first derivative of Figure 8. As shown, there are sharp, steep peaks within the range of the phase transition peaks in Figure 8. The y-axis has the first derivative of the heat flow, and the x-axis has the time of the cycle. The first derivative of HF can be considered as the thermal speed of TLCS.

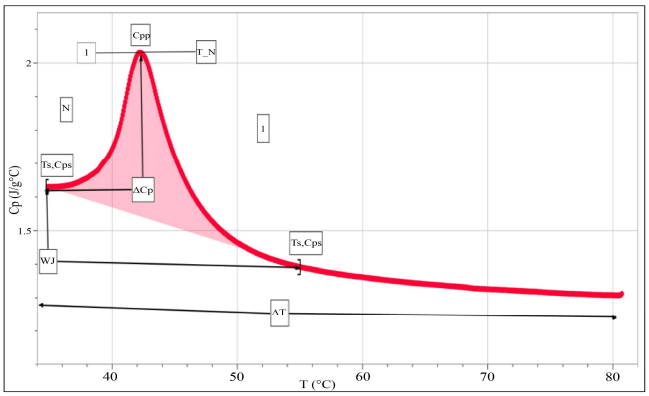

Fig. 6 The Cp Vs Temperature (T) for the endothermic nematic peak of the TLCS in heating.

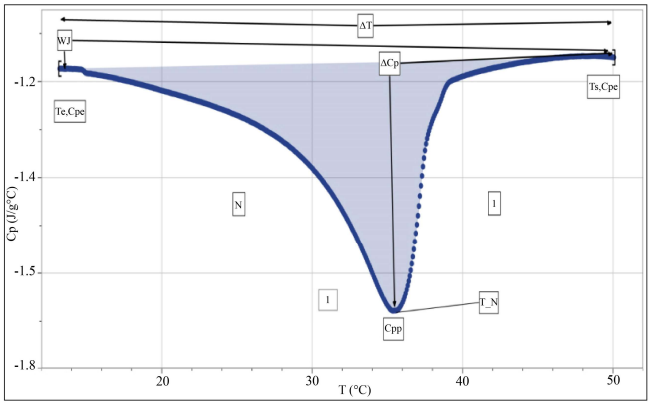

Fig. 7 The Cp Vs Temperature (T) for the exothermic nematic peak of the TLCS in cooling.

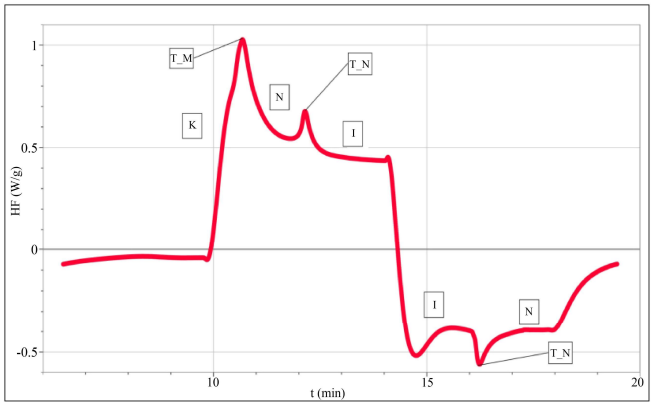

Fig. 8 Heat Flow Vs Time (t) plot for the heating and cooling of the TLCS.

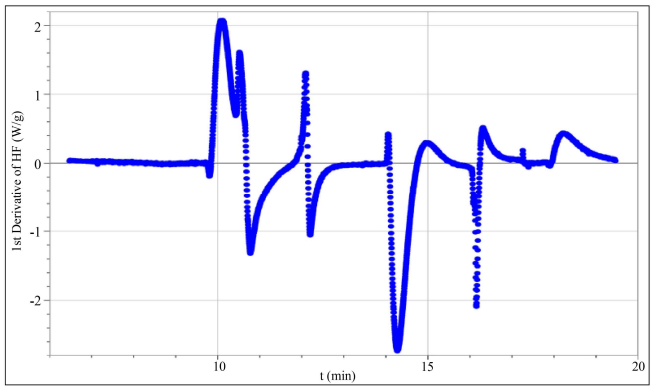

Fig. 9 The thermal speed vs time (min) plot for heating and cooling of TLCS.

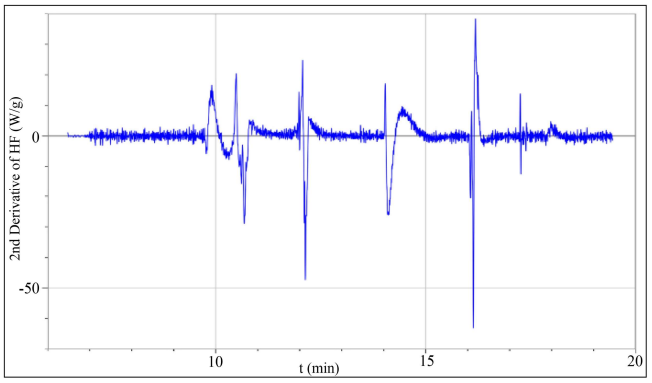

Fig. 10 The thermal acceleration vs time (min) for heating and cooling of TLCS.

Figure 10 shows the second derivative of Figure 8. As shown, the longest sharp peaks occur around the phase transition peaks in Figure 8. The y-axis is the second derivative of the heat flow, and the x-axis has the time of the cycle. It can be counted as the thermal acceleration of TLCS.

Figure 11 shows the third derivative of Figure 8. As shown, the longest sharp peaks occur around the phase transition peaks in Figure 8. The y-axis is the third derivative of the heat flow, and the x-axis has the time of the cycle. It can be counted as the thermal jerk of TLCS.

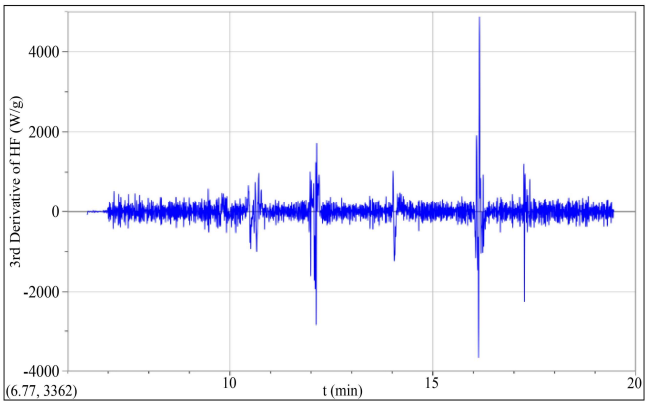

Fig. 11 The thermal jerk vs time (min) for heating and cooling of TLCS.

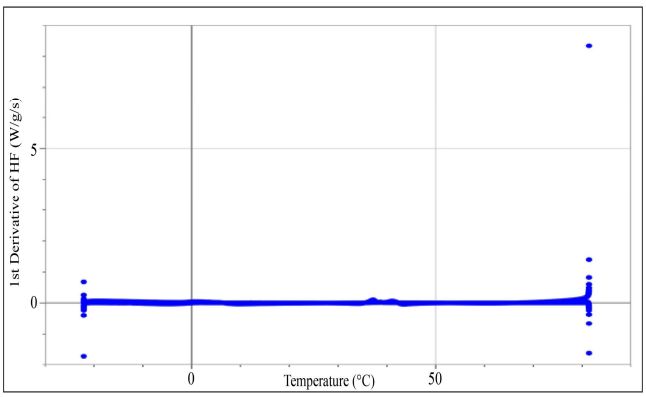

Fig. 12 The first derivative of HF (W/g/s) vs T (°C) for heating and cooling of TLCS.

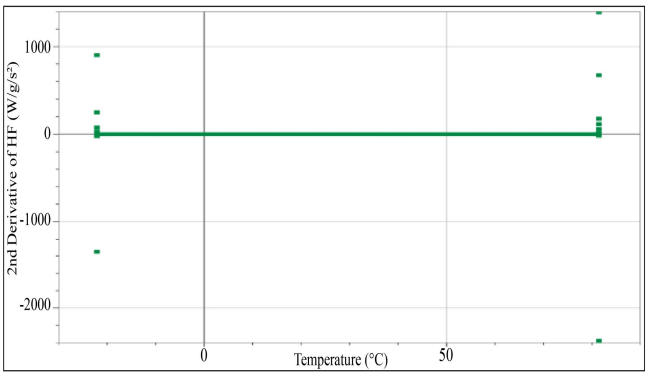

Fig. 13 The second derivative of HF vs T (°C) for heating and cooling of TLCS.

Figures 12, 13 and 14 show the details of the first, second and third derivatives of Figure 1. Figure 1 is plotted as HF vs T. It can be seen that the 1st, 2nd, and 3rd derivatives of HF show almost no features in the middle of the graph but just a flat line, but they do show some scattered data at the beginning and the end. It can be said that the data do not show any dynamics when plotted for derivatives from HF vs Temperature compared to the derivatives plotted from HF Vs time.

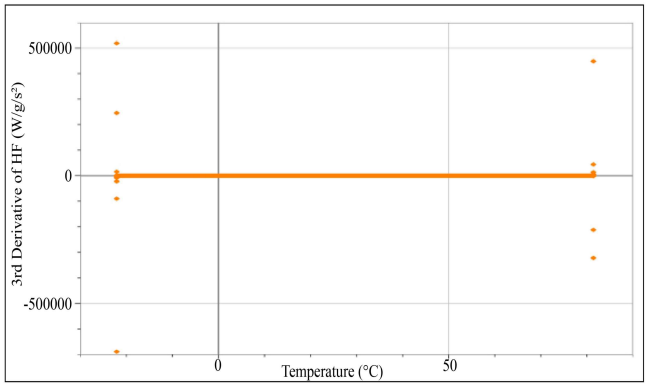

Fig. 14 The third derivative of HF vs T (°C) for heating and cooling of TLCS.

To see clear effects, the zoomed-in part of the heating of each separate transition is plotted for derivates from Figure 15 and onwards.

Figure 15 shows the first, second, and third derivatives of the heating of TLCS. The 1st left plot has the HF vs T of the heating phase transition peaks. The 1st right plot shows the 1st derivative of the endothermic phase transitions, the bottom left shows the 2nd derivative and the bottom right shows the 3rd derivative plots.

Figure 16 shows the first, second, and third derivatives of the melting phase transition peak of the TLCS.

Figure 17 shows the first, second, and third derivatives of the heat nematic phase transition peak of the TLCS. Figure 18 shows the first, second, and third derivatives of the cool nematic phase transition peak of the TLCS.

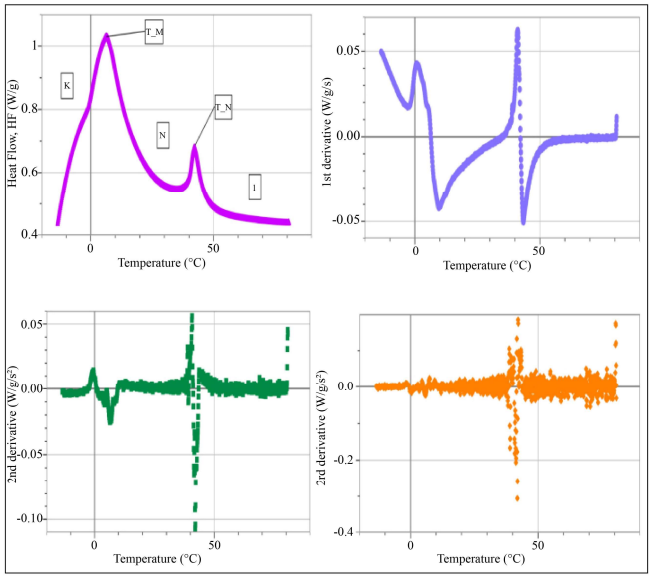

Fig. 15 Comparison of HF vs T phase transitions for heating shown for all three derivatives as a function of temperature for melting and nematic phase transitions of TLCS.

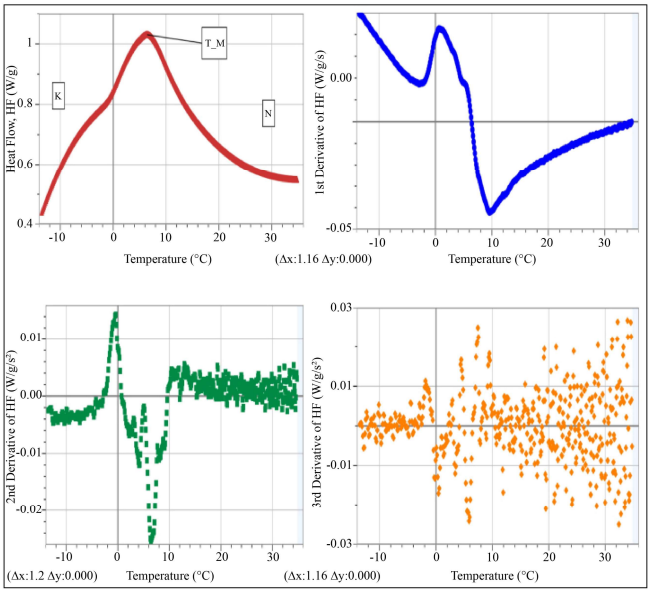

Fig. 16 The zoomed-in part of the melting transition is shown for all three derivatives of TLCS.

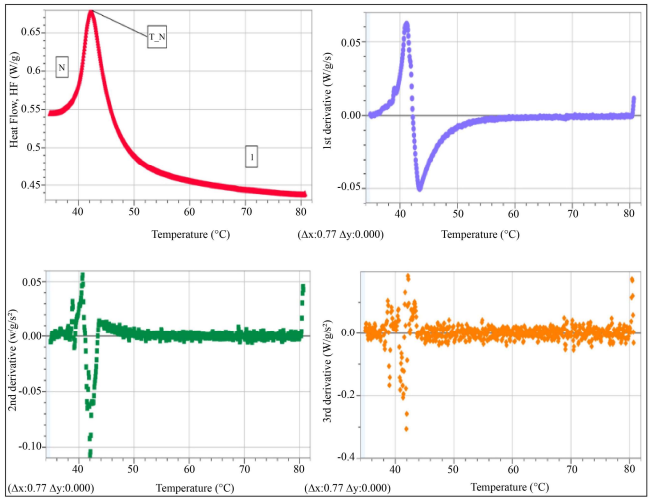

Fig. 17 Zoomed in part of heat nematic transition shown for all three derivatives for TLCS.

In all these three figures of 15, 16, 17, and 18, the protocol of the derivatives in the figures is as same as in Figure 15. The top left corner plot has the HF vs T plot; then the next top right plot shows the 1st derivative, the bottom left plot shows the 2nd derivative and the bottom right plot shows the 3rd derivative of TLCS.

Figures 19, 20, and 21 show the zoomed-in part of the first, second, and third derivatives of heat flow vs time plot for the melting phase transition peak, heat nematic peak, and the cool nematic peak of the TLCS. Different derivatives show different features in the graph representing the time dynamics of the TLCS of heat flow. The data obtained from the analyzed Logger Pro graphs are shown with details of each peak transition of TLCS in the data tables shown in Tables 1- 7.

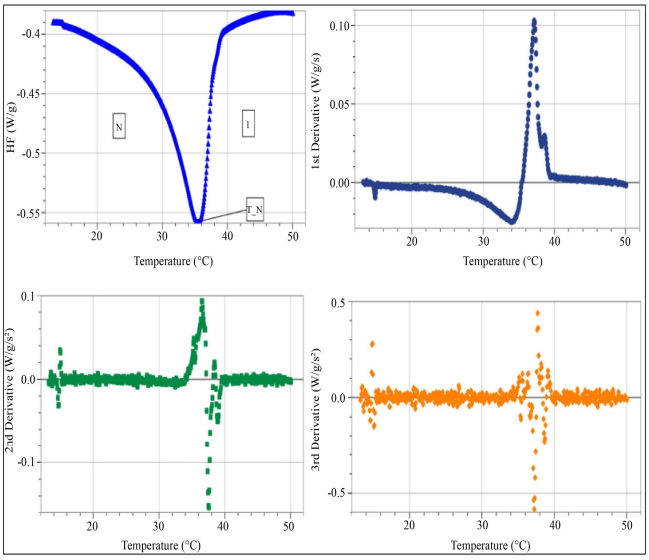

Fig. 18 The zoomed-in part of the cool nematic transition is shown for all three derivatives for TLCS.

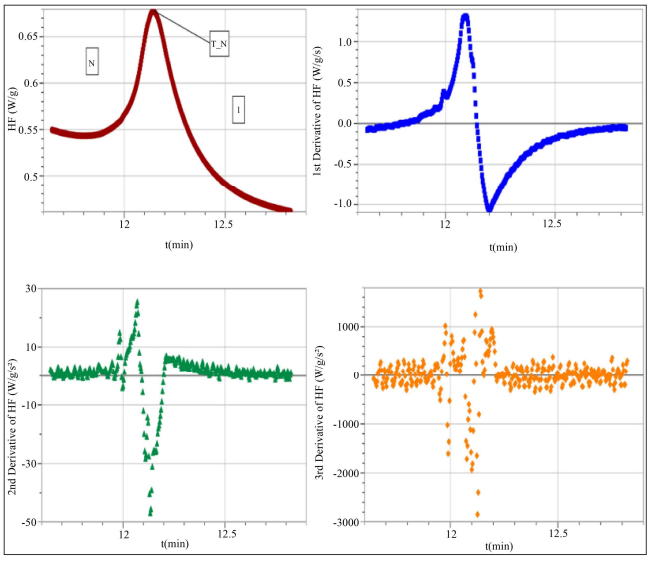

Fig. 20 Zoomed in part of HF vs t for heat nematic for all three derivatives of TLCS.

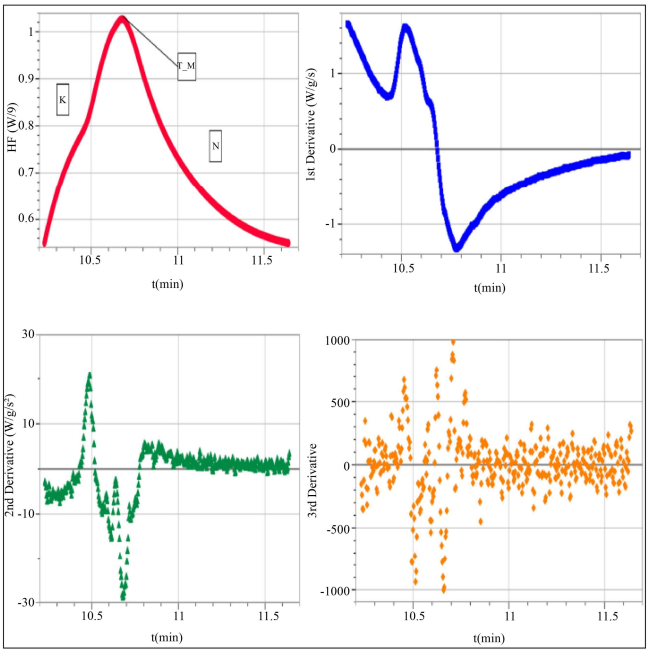

Fig. 19 The zoomed-in part of HF vs t for melting transition for all three derivatives for heating TLCS.

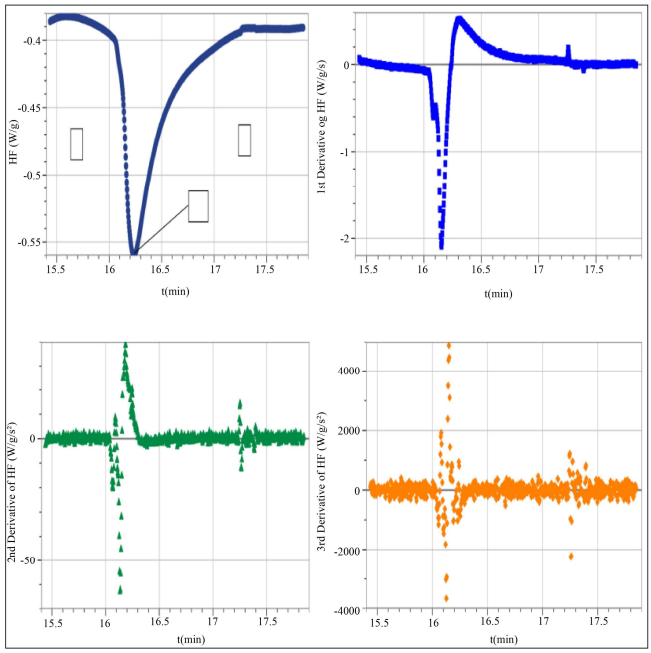

Fig. 21 The zoomed-in part of HF vs t for cool nematic for all three derivatives of TLCS.

5. Discussion

The Conclusions Figure 22 shows a mixture of three different liquid crystals resulting in the tails of the liquid crystals becoming tangled once the heat gets added and transitions to the isotropic state. Once they start heating up, the mixture transitions from crystalline (K) to nematic state (N). As the additional heat gets added, it transitions from the nematic (N) to the isotropic state (I). The Red molecule represents 7CB, the Green molecule represents 6CB, and the blue molecule represents 5CB.

Figure 23 shows that as the temperature gradually decreases, the liquid crystals transition from isotropic (I) to nematic states (N). When the temperature continues to decrease, the LC molecules cannot go back to the state of crystalline structure (K). The tails of the crystals are too entangled, which prevents the mixture from returning to the ordered crystalline state (K). It goes into a state called Frozen Nematic (F N).

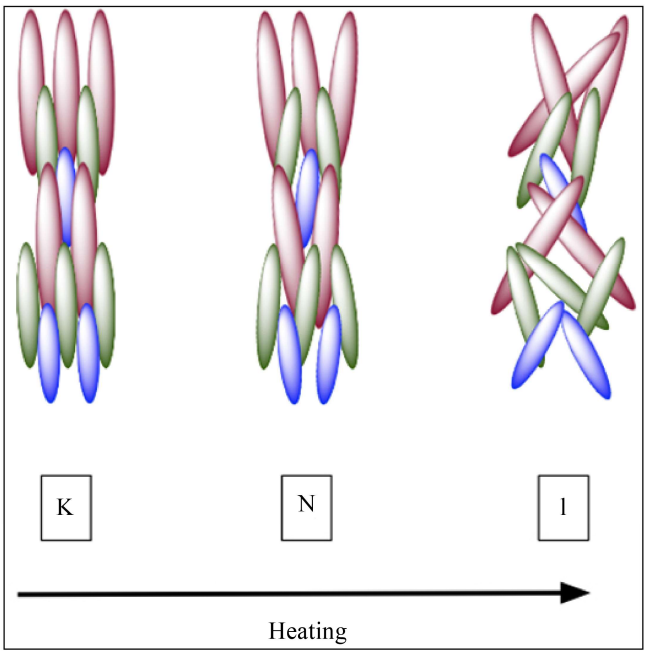

Fig. 22 Predicted Molecular orientation of 5CB, 6CB, and 7CB in TLCS during heating.

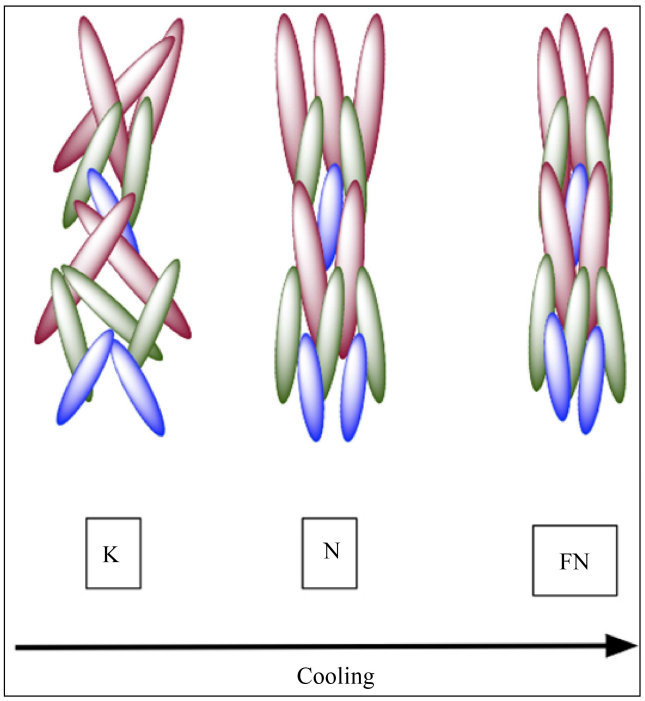

Fig. 23 Predicted Molecular orientation of 5CB, 6CB, and 7CB in TLCS during cooling.

Figures 24-26 display the summary of final data details endothermic and exothermic nematic Wing Jump, Cpp, and ΔCp comparison for the TLCS, BLCS, and pure compounds of 5CB, 6CB, and 7CB liquid crystals. The comparative data details can be seen in Tables from table 1-7. Figure 27 shows a comparative summary of graphs between BLCS and TLCS for the nematic range.

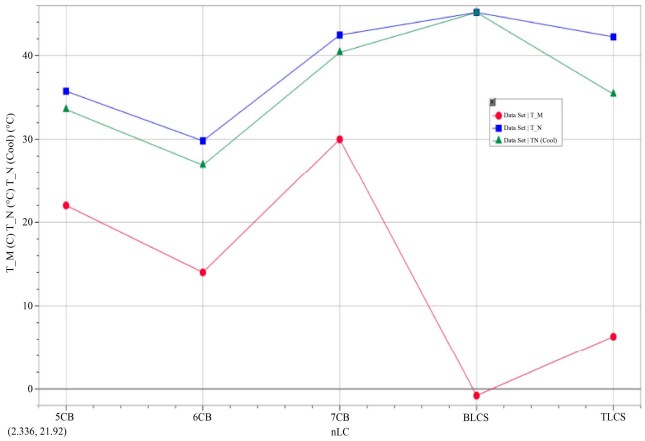

Fig. 24 Melting and Nematic transition temperatures of the TLCS, BLCS and pure component LCs 5CB, 6CB, and 7CB.

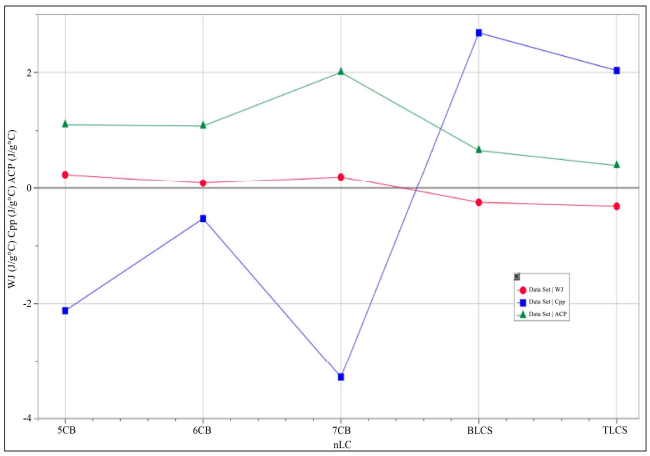

Fig. 25 Comparison of WJ, Cpp, and ΔCp in the endothermic nematic transition of the TLCS with BLCS and pure samples of 5CB, 6CB, and 7CB.

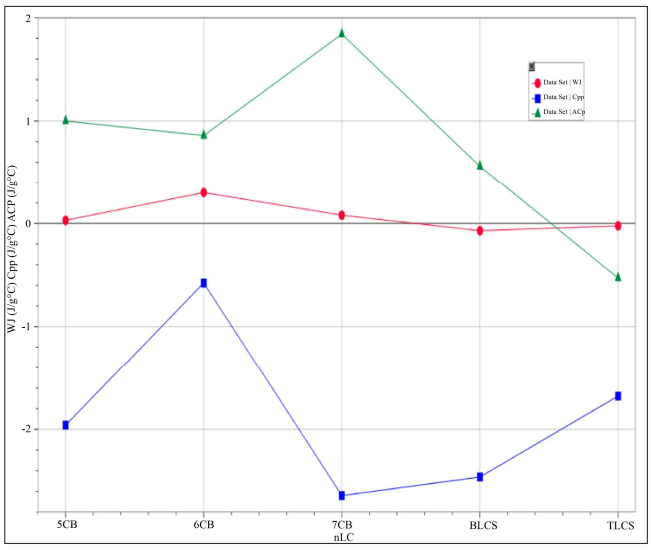

Fig. 26 Comparison of WJ, Cpp, and ΔCp in the exothermic nematic transition of the TLCS with BLCS and pure samples of 5CB, 6CB, and 7CB.

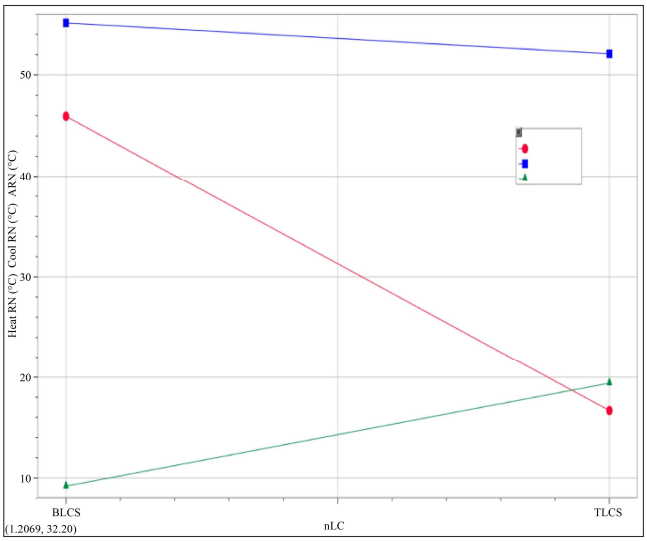

Fig. 27 Nematic range transition for the endothermic and exothermic transition of TLCS compared to BLCS.

Table 1 shows the comparison between 5CB + 6CB + 7CB TLCS and 5CB + 7CB BLCS of their crystalline to nematic (melting) transition. The TLCS requires less energy than BLCS for them. The melting point temperature for each of the pure compounds was obtained and recorded in Table 4. The BLCS and TLCS have a melting transition occurring at T_M = -0.79°C and T_M = 6.32°C. Table 2-3 contains the data values of endothermic and exothermic nematic transition for the LC samples. For the endothermic nematic transition, the TLCS had a lower enthalpy of 2.48 J/g in comparison to the other LCs. While the exothermic nematic transitions of the LCs showed that the TLCS had an enthalpy value of 4.36 J/g. The enthalpy for the cooling process was higher than 5CB and 6CB but lower than BLCS and 7CB. Table 5-6 contains the data values to compare with each nLC. When compared to the other LCs, TLCS has a lower WJ and ΔCp value for both the endothermic and exothermic transitions. During the endothermic nematic transition, the Cpp value of 2.0309 J/g°C for TLCS was higher in comparison to the single LCs. However, the Cpp values were lower compared to the BLCS Cpp value of 2.68 J/g°C. Table 7 shows a comparative study of the nematic range found for BLCS and TLCS. TLCS shows a shorter nematic range for heating but is larger in cooling when compared with BLCS. The change in the Nematic range between heat and cool can be seen as larger in TLCS from Table 7 and Figure 27.

From the data tables and summary graphs from Figures 24-27, TLCS shows some unique behavior not seen in single LCs or its parent LCs. It is also different from BLCS. The Nematic range found in TLCS is larger than BLCS and its parent LCs. The Nematic range is the important factor that decides whether LC can be used in LCD or not. The higher the Nematic range is, the higher chance it is to be used in LCDs. Based on our research of TLCS, we can say that the model we predicted for TLCS molecule between heating and cooling shows that TLCS molecules never go back to Crystalline and stays in Frozen Nematic when they are cooled after heating, making TLCS more important in the LCD world.

6. Data Tables

Table 1. Melting to Nematic Transition Temperatures of the TLCS compared to binary liquid crystal mixture of 5CB and 7CB.

Melting Transition peak									
Sample	T_s (°C)	T_e (°C)	ΔT(°C)	Cp_s (J/g°C)	Cp_e (J/g°C)	Cp_p (J/g°C)	ΔCp(J/g°C)	ΔH(J/g)	WJ (J/g°C)
5CB+6CB+7CB	-13.497	34.7651	48.2621	1.3031	1.6298	3.079	0.3267	34.05	0.3267
5CB+7CB [10]	-26.33	34.24	60.57	-0.05	2.28	3.6	1.32	93.38	2.33

Table 2. Nematic to Isotropic Transition Temperatures of the TLCS compared to pure component 5CB, 6CB, and 7CB LCs and the binary liquid crystal mixture of 5CB and 7CB.

Endothermic Nematic Transition Peak									
Sample	T_s (°C)	T_e (°C)	ΔT(°C)	Cp_s (J/g°C)	Cp_e (J/g°C)	Cp_p (J/g°C)	ΔCp(J/g°C)	ΔH(J/g)	WJ (J/g°C)
5CB+6CB+7CB	34.8374	80.72	45.8826	1.6298	1.3121	2.0309	0.4011	2.48	-0.31767
5CB+7CB [10]	36.42	63.71	27.29	2.27	2.02	2.68	0.66	3.39	-0.25
5CB [12]	30.12	40.59	10.45	2.98	3.22	-2.12	1.10	221.8	0.24
6CB [12]	25.55	39.79	14.23	1.52	1.61	-0.53	1.08	158.4	0.09
7CB [12]	38.71	46.71	7.94	1.47	1.27	-3.28	2.00	99.46	0.20

Table 3. Isotropic to Nematic Transition Temperatures of the TLCS sample compared to pure component 5CB, 6CB, and 7CB LCs and the binary liquid crystal mixture of 5CB and 7CB.

Exothermic Nematic Transition Peak									
Sample	**T_s (°C)**	**T_e (°C)**	**ΔT(°C)**	**Cp_s (J/g°C)**	**Cp_e (J/g°C)**	**Cp_p (J/g°C)**	**ΔCp(J/g°C)**	**ΔH(J/g)**	**WJ (J/g°C)**
5CB+6CB+7CB	50.0681	13.2042	-36.8639	-1.1498	-1.1731	-1.6784	-0.5286	4.36	-0.0233
5CB+7CB [10]	42.34	20.68	63.02	-1.90	-1.97	-2.46	0.56	4.57	-0.07
5CB [12]	39.26	23.77	15.5	2.93	2.96	-1.96	1.00	1.62	0.03
6CB [12]	36.85	21.02	15.8	1.40	1.10	-0.576	0.859	1.20	0.30
7CB [12]	45.61	30.28	15.33	0.80	0.88	-2.64	1.84	8.33	0.08

Table 4. Melting and nematic transition for endothermic and exothermic phase transitions.

nLC	T_M (°C)	Heat T_N (°C)	Cool T_N (°C)
5CB [12]	22	35.75	33.56
6CB [12]	14	29.82	26.92
7CB [12]	30	42.45	40.37
BLCS [10]	-0.79	45.15	45.15
TLCS	6.32	42.2322	35.4

Table 5. Comparison of WJ, Cpp, and ΔCp for the nLC samples in the endothermic nematic state.

nLC	WJ (J/g°C)	Cpp (J/g°C)	ΔCp (J/g°C)
5CB [12]	0.24	-2.12	1.1
6CB [12]	0.09	-0.53	1.08
7CB [12]	0.2	-3.28	2
BLCS [10]	-0.25	2.68	0.66
TLCS	-0.31767	2.0309	0.4011

Table 6. Comparison of WJ, Cpp, and ΔCp for the nLC samples in the exothermic nematic state.

nLC	WJ (J/g°C)	Cpp (J/g°C)	ΔCp (J/g°C)
5CB [12]	0.03	-1.96	1
6CB [12]	0.3	-0.576	0.859
7CB [12]	0.08	-2.64	1.84
BLCS [10]	-0.07	-2.46	0.56
TLCS	-0.0233	-1.6784	-0.5286

Table 7. Comparison of the nematic range for heating and cooling the samples (BLCS and TLCS).

nLC	Heat R_N (°C)	Cool R_N (°C)	dR_N (°C)
BLCS [10]	45.94	55.12	9.18
TLCS	35.91	55.40	19.41

7. Conclusion

This paper shows a combination of three different liquid crystals. The DSC techniques were used to analyze the phase transitions of the TLCS. To achieve a tertiary liquid crystal system, three different LCs were mixed with a 1:1:1 ratio. The TLCS was heated and cooled in the range of -40°C to 80°C. The results of the study revealed that the three different liquid crystals exhibited a completely different state than their single counterparts. The research concluded that the TLCS exhibited two phases: endothermic and exothermic. The data shows that there are melting and nematic transitions that occur during the heating, while there was only a nematic transition that occurred during the cooling process. When TLCS was cooled to a lower temperature, it didn't ever return to the crystalline state due to the entangling of the tails. Based on the results, TLCS could be used for LCDs because their Nematic Range occurs at a lower temperature. The study's results can help researchers understand how mixing different liquid crystals can affect phase transitions.

Acknowledgments

We are thankful to Professor John C. MacDonald from the Department of Chemistry, Biochemistry and Life Sciences and Bioengineering Center at WPI, Worcester, MA, USA DSC instrument. We are also thankful to NETZSCH company for DSC 214 pans and lids. The student, Medaelle, would like to thank Dr. Dipti Sharma for supervising a senior research internship working with TLCS materials and Emmanuel College for Logger Pro.

References

[1] The Kent State University website, Advanced Materials and Liquid Crystal Institute. [Online]. Available: https://www.kent.edu/amlci/what-are-liquid-crystals#:~:text=What%20you%20see%20in%20this%20small%20glass%20vial,disappears%2C%20rapidly%20taken%20over%20by%20a%20clear%20liquid

[2] The Chemistry LibreTexts website, 2020. [Online]. Available: https://chem.libretexts.org/Bookshelves/Physical_and_Theoretical_Chemistry_Textbook_Maps/Supplemental_Modules_(Physicaland_Theoretical_Chemistry)/Physical_Properties_of_Matter/States_of_Matter/Liquid_Crystals

[3] The Wikipedia website. [Online]. Available: https://en.wikipedia.org/wiki/Liquid_crystal

[4] K. G. Neerajakshi, "Thermodynamic and Acoustic Properties of Binary Mixtures of PEGDME 200 with 1-Propanol," *SSRG International Journal of Applied Chemistry*, vol. 7, no. 3, pp. 33-37, 2020. [CrossRef] [Publisher Link]

[5] The Imperial College London. [Online]. Available: https://www.ch.ic.ac.uk/local/projects/abbott/LCDs.htm

[6] The Lifewire Website, 2022. [Online]. Available: https://www.lifewire.com/what-is-liquid-crystal-display-lcd-2625913

[7] The Nelson Miller website. [Online]. Available: https://nelson-miller.com/nematic-vs-smectic-phase-in-lcds/

[8] The Linseis website, 2020. [Online]. Available: https://www.linseis.com/en/methods/differential-scanning-calorimetry-dsc/

[9] P.J. Haines, M. Reading, and F.W. Wilburn, "Differential Thermal Analysis and Differential Scanning Calorimetry," *Handbook of Thermal Analysis and Calorimetry,* vol. 1, pp. 279-361, 1998. [CrossRef] [Google Scholar] [Publisher Link]

[10] Mathew C. Doran, and Dipti Sharma. "Melting and Nematic Phase Transitions of a Next Generation "Binary Liquid Crystal System (BLCS)" 5CB+7CB using Logger Pro," *International Journal of Research in Engineering and Science (IJRES)*, vol. 10, no. 12, pp. 462-483, 2023. [Google Scholar] [Publisher Link]

[11] K. P. Sigdel, and G. S. Iannacchione, "Evolution of the Isotropic to Nematic Phase Transition in Binary Mixtures of Octylcyanobiphenyl and n-Hexane," *The Journal of Chemical Physics,* vol. 133, no. 4, 2010. [CrossRef] [Google Scholar] [Publisher Link]

[12] M. Seide, M. C. Doran, and D. Sharma, "Analyzing Nematic to Isotropic (N-I) Phase Transition of nCB Liquid Crystals Using Logger Pro," *European Journal of Applied Sciences*, vol. 10, no. 3, pp. 98-124, 2022. [CrossRef] [Google Scholar] [Publisher Link]

[13] G. A. Oweimreen, and M. A. Morsy, "DSC Studies on P-(N-alkyl)-p′-Cyanobiphenyl (RCB's) and P-(N-Alkoxy)-p′-Cyanobiphenyl (ROCB's) Liquid Crystals," *Thermochimica Acta ,* vol. 346, no. 1-2, pp. 37-47, 2000. [CrossRef] [Google Scholar] [Publisher Link]

[14] Shailendra Kumar, and Priya Bisht, "Using Evacuated Tube Collectors (ETC) as Micro-Encapsulation for Thermal Energy Storage: Comparative Charging-Discharging Characteristics of a Phase Change Material (PCM) and Water," *SSRG International Journal of Mechanical Engineering*, vol. 8, no. 2, pp. 12-17, 2021. [CrossRef] [Google Scholar] [Publisher Link]

[15] Dipti Sharma, John C. MacDonald, and Germano S. Iannacchione, "Thermodynamics of Activated Phase Transitions of 8CB: DSC and MC Calorimetry," *The Journal of Physical Chemistry B,* vol. 110, pp. 16679-16684, 2006. [CrossRef] [Google Scholar] [Publisher Link]

[16] Mathew C. Doran, and Dipti Sharma, "Plotting DSC Results using Logger Pro for a Binary Liquid Crystal System (BLCS)," *International Journal of Research in Engineering and Science*, vol. 10, no.12, pp. 449-461, 2022. [Google Scholar] [Publisher Link]

[17] Mathew C. Doran, and Dipti Sharma, "Effect of Ramp Rates on Phase Transitions of a Next Generation 'Binary Liquid Crystal System' (BLCS) 5CB+7CB," *International Journal of Engineering Inventions*, vol. 12, no. 1, pp. 291-306, 2023. [Publisher Link]

[18] J. Mello and D. Sharma, "Crystal Growth, Percent Crystallinity and Degree of Crystallization of 5OCB Liquid Crystal (Analyzing using Logger Pro)," *International Journal of Engineering Inventions*, vol. 12, no. 1, pp. 166-285, 2023. [Publisher Link]

[19] Juliana Mello, and Dipti Sharma, "Effect of Reheating and Ramp Rates on Phase Transitions of 5OCB Liquid Crystal using Logger Pro," *International Journal of Research in Engineering and Science*, vol. 10, no. 9, pp. 218-236, 2022. [Google Scholar] [Publisher Link]

[20] J. Mello, and D. Sharma, "Details of Nematic Phase Transition and Nematic Range of 5OCB Liquid Crystal using Logger Pro," *International Journal of Research in Engineering and Science*, vol. 10, no. 9, pp. 197-217, 2022. [Google Scholar] [Publisher Link]

[21] Dipti Sharma, and Kim Farah "A Review of Nematic Liquid Crystals," *Trends in Physical Chemistry*, vol. 16, pp. 47-52, 2016. [Publisher Link]

[22] Dipti Sharma, and Kim Farah, "Determination of Latent Heat of Phase Transitions of 8CB Liquid crystal," *Trends in Physical Chemistry*, vol. 16, pp. 17-24, 2016. [Publisher Link]

[23] Yuan Shen, and Ingo Dierking, "Perspectives in Liquid-Crystal-Aided Nanotechnology and Nanoscience," *Applied Scienes*, vol. 9, no. 12, pp. 2512, 2019. [CrossRef] [Google Scholar] [Publisher Link]

[24] Pritam Kumar Jana et al, "Entropy-Driven Impurity-Induced Nematic-Isotropic Transition of Liquid Crystals," *arXiv*, pp. 1-6, 2019. [CrossRef] [Google Scholar] [Publisher Link]

[25] D. Sharma, "A Non-Isothermal Activated Kinetics of K-SmA Transition of the Aligned Octylcyanobiphenyl," *Journal of Thermal Analysis and Calorimetry*, vol. 109, no. 1, pp. 331-335, 2011. [CrossRef] [Google Scholar] [Publisher Link]

[26] The New Vision Display website, 2018. [Online]. Available: https://www.newvisiondisplay.com/liquid-crystal/

[27] D. Sharma, "Calorimetric Study of Activated Kinetics of the Nematic and Smectic Phase Transitions in an Aligned Nano-Colloidal Liquid Crystal+Aerosil Gel," *Journal of Thermal Analysis and Calorimetry*, vol. 93, no.3, pp. 899-906, 2008. [CrossRef] [Google Scholar] [Publisher Link]